

ON THE PROBABILITY OF GENERALIZED CORRELATION FUNCTIONS

Manfred Ehlers
 Institute of Photogrammetry and Engineering Surveys
 University of Hannover
 Commission III, WG II/5

ABSTRACT

A great problem - especially in images with low signal-to-noise ratio (SNR) - is the failure of the correlation function. In this paper four different objective functions for the correlation process are compared in a statistical test on identical images with added random noise of different magnitudes. An analytical formula for the correlation probability depending on image SNR is derived for each objective function. Methods for SNR estimation in images with unknown noise are presented. One main result is that in imagery of low SNR other functions than the normal correlation function should be applied. Highest correlation probability shows the phase correlation method.

Introduction

One central problem in remote sensing and photogrammetry is the automation of the human eye's capability especially the stereoscopic viewing and object identification. The digital computer controlled solution of this problem leads to correlation techniques. The notation "correlation" is used in a generalized sense as a method for point or object identification. Therefore different objective functions for the correlation process are thinkable and already in practical use (EHLERS, 1982b).

In photogrammetry these parallaxes can be used to derive a terrain model or to produce an orthophoto; in remote sensing they serve for image rectification or change detection. For the latter case the Institute of Photogrammetry at Hanover University developed the software correlation-rectification system DISCOR (DISCOR = Digital software correlator for image rectification) (EHLERS, 1983).

One main disadvantage in correlation process is the possibility of incorrect parallax calculation, especially in images with a low signal-to-noise ratio (SNR). In photogrammetry the influence of image noise on the correlation or pointing precision has been investigated for instance by FÖRSTNER 1982 or TRINDER 1982. On the other hand in remote sensing the main problem is not the precision, but the probability of the correlation function. Due to different sensors, different scales and different recording conditions of remote sensing imagery the identification of homologous points is very difficult. Remotely sensed images are often contaminated by noise and have to be pre-processed before further evaluation (EHLERS, 1982a). An example is given in fig.1-3.

Fig.1 shows a photogrammetric image (frame camera) of the city of Cologne (Federal Republic of Germany). Fig.2 and 3 show the same part in LANDSAT and SEASAT imagery. Especially the SEASAT-radar channel contains a high noise level. In order to avoid noise induced miscorrelation, functions other than the 'normal' correlation function have been proposed (PRATT, 1974; KUGLIN and HINES, 1975; BAILEY et al., 1976; EHLERS, 1982b).

In this paper the effect of image quality on the correlation probability will be investigated to estimate the connection between both variables. One main aim here is to determine the correlation function with the smallest probability of failure. This is tested with four different objective functions in an empirical-statistical manner on the DISCOR system that is part of the Hannover digital image processing system MOBI-DIVAH (DENNERT-MÖLLER et al., 1982).



Fig.1: Aerial photography (frame camera)

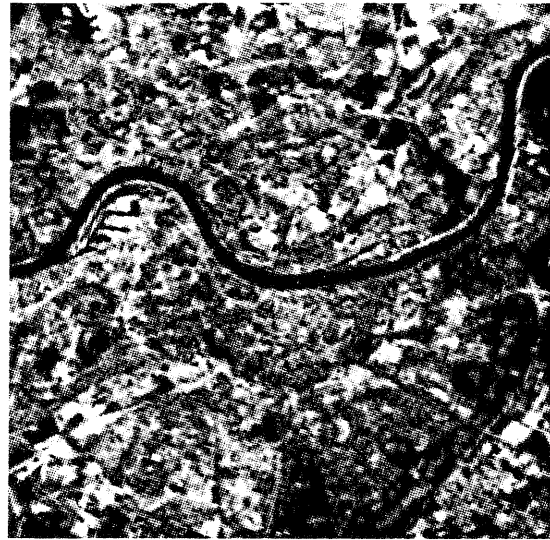


Fig.2: LANDSAT MSS image

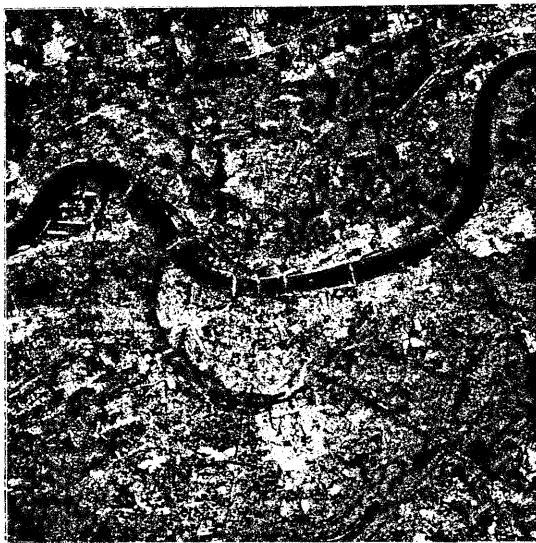


Fig.3: SEASAT radar image

Mathematical Basis

Image and noise model

In remote sensing the ground signal is changed before and during the recording process. The original image signal $g(x,y)$ is disturbed by various influences, e.g. atmosphere, intensity of light, sensor sensitivity, digitization etc. Errors due to these reasons can be divided into recording (including atmospheric effects) and quantization errors. In the following we assume that atmospheric and recording processes add random noise n' to the original signal. Thus the recorded signal g' can be written as

$$g'(x,y) = g(x,y) + n'(x,y) \quad (1)$$

Analog/digital transformation produces two effects. The finite scanning aperture size causes low pass filtering with a filter function h'' superposed with additional electronic

noise [CASTLEMAN 1979].

$$g''(x,y) = g' * h''(x,y) + n''(x,y) \quad (2)$$

setting (1) into equation (2) the digitized signal g'' can be written as

$$g''(x,y) = g * h(x,y) + n(x,y) \quad (3)$$

using the abbreviations $n = n' * h'' + n''$ and $h \equiv h''$.

Hence the digitized image signal g'' consists of a filtered deterministic part $g * h$ and a stochastic component n .

Correlation model

Following (3) two independent recorded and sampled images of the same area can be written as

$$g_1'' = g * h_1 + n_1 \quad (4)$$

$$g_2'' = g * h_2 + n_2$$

Aim of the generalized correlation is to derive unknown geometric transformation between g_1'' and g_2'' .

Usually this is done by minimizing an objective function that measures the distance between the grey values in small subimages, the correlation windows. Additionally an image transformation can be possible. So objective functions for the detection of identical points consist of a function M ('metrics') for distance measurement and a transformation parameter T for image preprocessing. An often used function for instance is the sum of squared differences between the grey values. T can change the image signal (e.g. filtering) and/or the coordinates (e.g. considering different perspectives). The task of the objective function is to find $(\Delta x, \Delta y)$, so that M will be minimized:

$$M \{T(g_1''(x,y), T(g_2''(x + \Delta x, y + \Delta y)))\} = \text{Minimum}_{\Delta x, \Delta y} \quad (5)$$

Objective functions

As at the evaluation of remote sensing imagery (especially from satellites) usually terrain differences and perspectives can be neglected [KONECNY, 1976], in the following the transformation parameter T only effects the image intensities considering no geometric conditions. With this simplification four correlation functions are integrated into the DISCOR system:

- a) The 'normal' product moment correlation coefficient which is equivalent to a square [Gaussian] metrics. The transformation operator is the identity operator.
- b) The correlation intensity coefficient, which has been derived from coherent optical considerations. The image signals are mapped onto the complex plane and the intensity of the complex correlation function is computed. The coefficient is weighted by a parameter p depending on the variances in the correlation windows. The metrics M again is Gaussian, the transformation operator T is the complex exponentiation [GÖPFERT, 1980].
- c) The Laplace coefficient, i.e. the same of the absolute differences of the image signals with an absolute [Laplacian] metrics M and the identity operator T .
- d) The phase correlation coefficient, i.e. the inverse Fourier transform of the norma-

lized cross spectrum of both images. Hence only the phase differences are considered. M again is Gaussian. T normalizes the cross spectrum in the frequency domain (KUGLIN and HINES, 1975).

It can be shown by using Fourier transform theorems that the functions a) and d) are special cases of a generalized filtered correlation function (EHLERS, 1983).

Table 1 lists the objective functions, their one dimensional unnormalized mathematical expression, the metrics M and the transformation parameter T. The symbols $(.)^2$ and $|\cdot|$ stand for Gaussian and Laplacian metrics respectively.

Table 1: DISCOR objective functions for correlation

| Objective function | Math.expression (unnormalized) | Metrics | T-Operator |
|---|---|-----------|--------------------------------|
| a) product moment correlation coefficient | $\int_{-\infty}^{\infty} g_1(x)g_2(x + \Delta x)dx$ | $(.)^2$ | $T(g(x)) = g(x)$ |
| b) intensity coefficient | $\int_{-\infty}^{\infty} \cos p_1(g_1(x)-g_2(x + \Delta x))dx)^2$ + $\int_{-\infty}^{\infty} \sin p_1(g_1(x)-g_2(x + \Delta x))dx)^2$ | $(.)^2$ | $T(g(x)) = e^{-jP \cdot g(x)}$ |
| c) Laplace coefficient | $\int_{-\infty}^{\infty} g_1(x)-g_2(x + \Delta x) dx$ | $ \cdot $ | $T(g(x)) = g(x)$ |
| d) phase correlation coefficient | $\int_{-\infty}^{\infty} \frac{G_1^*(f)G_2(f)}{ G_1^*(f)G_2(f) } e^{2\pi j f \Delta x} df$ | $(.)^2$ | $T(G(f)) = \frac{1}{ G(f) }$ |
| | $[G(f) = \text{Fourier transform of } g(x):$ $G(f) = \int_{-\infty}^{\infty} g(x) \cdot e^{-2\pi j f x} dx \text{ with } j = \sqrt{-1}]$ | | |

In the following chapter the correlation probability is studied on statistical tests with different artificial noise distributions.

Correlation Probability and SNR

Image material

As test image a digitized section of an aerial photograph with an original scale of 1:50 000 has been chosen (fig.4). Due to the high SNR in photogrammetric pictures this image is used to simulate an undisturbed original ground signal. It is assumed to be noise-free. Now random noise in different magnitudes and distributions is added to the reference signal according to (3). The mean SNR in the noisy images can be estimated by

$$\text{SNR} = \frac{\sigma_g}{\sigma_g} \quad (5)$$

where $\overline{\sigma_g}$ is the mean value for standard deviation of image signal and $\overline{\sigma_n}$ is random noise mean standard deviation. The test has been executed with 20 different image noise levels with an SNR ranging from 60.8 to 0.8. The noise was Gaussian and uniform distributed.

Fig.5 and 6 show two noisy images with an SNR = 2.6 and 1.0 respectively.



Fig.4: Reference image (noise-free)

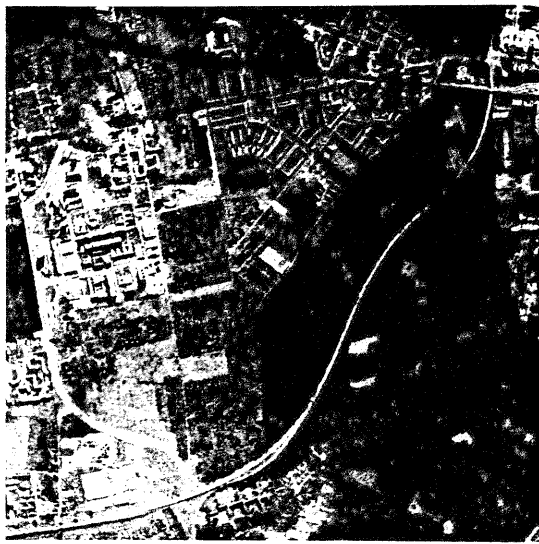


Fig.5: Search image (SNR = 2.6)



Fig.6: Search image (SNR = 1.0)

The differences can be seen more clearly in fig.7, showing the same line in the reference and the two disturbed images.

In the reference image 20 correlation test points have been chosen on the digital DIVAH screen. The correlation points are the centers of 11 x 11 pattern matrices. In the noisy images the corresponding search matrices have the same center coordinates and a size of 30 x 30 pixel. Within these windows the correlation coefficients for all possible pattern matrix positions are computed. With the a priori knowledge for correct correlation we can estimate the correlation probability for every objective function. Fig.8 shows the reference image with the bordered pattern matrices.

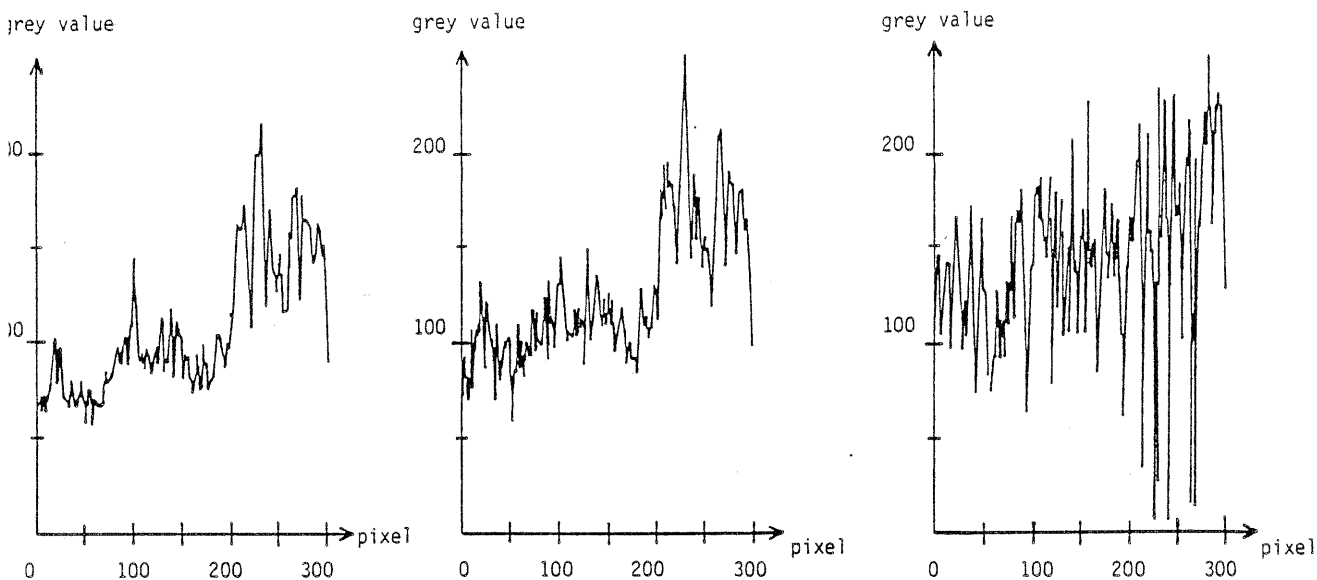


Fig.7: Line in reference image (left), image with SNR = 2.6 (middle) and image with SNR = 1.0 (right)

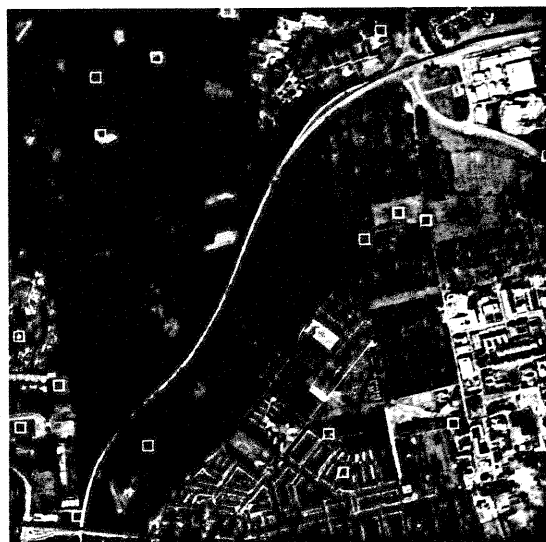


Fig.8: Reference image with correlation points

Test results

The correlation test shows no significance on the applied kind of noise distribution so that we can combine all the results. Only the SNR values are considered.

The SNR is computed in every correlation window and summarized in 18 different SNR classes. In each class the correlation probability for every objective function is calculated. The result can be seen in table 2. A probability of 0.5 for instance means that 50 % of the correlation points in the corresponding SNR class have been recognized correctly.

Tab.2: Correlation probability and SNR

| SNR | Probability with objective function ^{+)J} | | | |
|---------|--|------|------|------|
| | a | b | c | d |
| < 0.10 | 0.00 | 0.00 | 0.00 | 0.00 |
| 0.13 | 0.00 | 0.00 | 0.00 | 0.36 |
| 0.18 | 0.06 | 0.12 | 0.00 | 0.47 |
| 0.25 | 0.44 | 0.17 | 0.00 | 0.67 |
| 0.31 | 0.44 | 0.38 | 0.00 | 0.63 |
| 0.39 | 0.57 | 0.57 | 0.00 | 0.93 |
| 0.43 | 0.71 | 0.79 | 0.00 | 0.86 |
| 0.49 | 0.62 | 0.69 | 0.15 | 0.77 |
| 0.57 | 0.88 | 0.94 | 0.06 | 1.00 |
| 0.66 | 0.88 | 0.88 | 0.00 | 0.94 |
| 0.76 | 1.00 | 1.00 | 0.17 | 1.00 |
| 0.86 | 0.94 | 1.00 | 0.24 | 1.00 |
| 0.96 | 0.92 | 1.00 | 0.25 | 1.00 |
| 1.25 | 1.00 | 1.00 | 0.33 | 1.00 |
| 1.75 | 1.00 | 1.00 | 0.63 | 1.00 |
| 3.50 | 1.00 | 1.00 | 0.95 | 1.00 |
| 7.50 | 1.00 | 1.00 | 0.98 | 1.00 |
| > 10.00 | 1.00 | 1.00 | 1.00 | 1.00 |

- +) a = product moment correlation coefficient
 b = intensity coefficient (global variances)
 c = Laplace coefficient
 d = phase correlation coefficient

For an easier interpretation it is convenient to develop a mathematical expression of the relationship between probability and SNR.

Mathematical approximation of correlation probability and SNR

To obtain an analytical expression of the connection between noise and correlation probability P , the P -values are plotted versus the corresponding logarithmic SNR. We get an S-shaped curve with an almost linear increase in the medium domain (see fig.9). For an analytical formulation we have to approximate the probability functions considering the boundary conditions

$$\lim_{SNR \rightarrow 0} p = 0$$

$$SNR \rightarrow 0$$

and

$$\lim_{SNR \rightarrow \infty} p = 1$$

$$SNR \rightarrow \infty$$

An easy analytical solution can be given by the 'logistic growth curve'

$$y = \frac{1}{1 + e^{-a_1 x - a_0}} \quad (6)$$

which has been set up first by VOLTERRA for population processes (WHISTON, 1974).

For the estimation of the parameters a_0 and a_1 we consider the expression $\log \frac{y}{1-y}$ of equation (6):

$$\log \frac{y}{1-y} = \log y - \log (1-y) = a_1 x + a_0$$

in our case

$$\log \frac{P}{1-P} = a_1 \log \text{SNR} + a_0 \quad (7)$$

Fig.9 shows the approximated curves $P(\text{SNR})$ for all objective functions according to (7). Also their 95 % confidence interval and the measured probabilities \hat{p} are plotted. The significance of the fits has been verified by chi-square-testing.

Objective function classification

To classify the correlation functions limiting values are extracted from fig.9. The parameter $S_{0.05}$, $S_{0.50}$ and $S_{0.95}$ denote the SNR with a probability of 5 %, 50 % and 95 % respectively. Table 3 presents the estimated parameters with their upper 95 % confidence interval.

Table 3: SNR values with $P = 0.05, 0.5$ and 0.95

| Objective function | $S_{0.05}$ | 95 % confidence | $S_{0.50}$ | 95 % confidence | $S_{0.95}$ | 95 % confidence |
|--------------------|------------|-----------------|------------|-----------------|------------|-----------------|
| a | 0.14 | 0.24 | 0.34 | 0.50 | 0.82 | 1.40 |
| b | 0.15 | 0.26 | 0.34 | 0.40 | 0.76 | 1.25 |
| c | 0.42 | 0.76 | 1.40 | 2.20 | 4.60 | 12.00 |
| d | 0.06 | 0.12 | 0.19 | 0.28 | 0.50 | 1.00 |

The classification criteria listed in table 3 allow us to come to the following conclusions:

- (i) Best correlation probability is shown by the phase correlation method d). A SNR of 1.5 or lower in our images requires the application of this objective function to achieve most probable correlation.
- (ii) The objective functions a) and b) have almost the same probability of correct correlation showing no significant differences. So other criteria (e.g. precision or computation time) may decide which one has to be used. If image SNR is above 1.5, functions a), b) and d) can be employed without preference.
- (iii) A poor probability is associated with function c), the Laplace coefficient. Wrong correlation even occurs at an image SNR of 9.0. Although a very fast function (BAILEY et al., 1976), it shows insufficient probability and should therefore be handled with care in the correlation process.

With these limiting values it is possible to control the application of objective functions in an automatic manner. If the SNR is known, it is possible to decide which correlation function can be chosen and to estimate the according a priori correlation probability. So the image SNR is all an automatic correlation controller has to know. But how can this be calculated if image and noise are almost inseparable ?

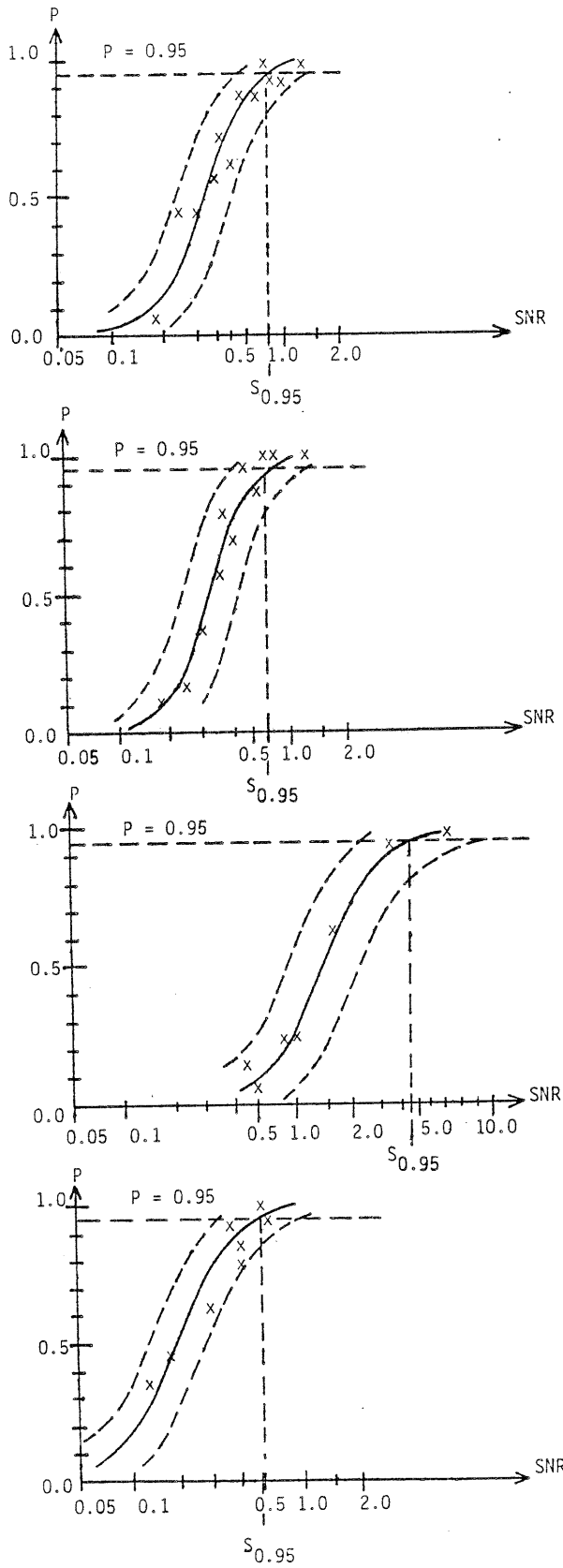


Fig.9: Probability and SNR of product moment correlation coefficient a), intensity coefficient b), Laplace coefficient c) and phase correlation coefficient d) [from top to bottom]

Estimation of image SNR

The crucial point of all investigation is to find a good SNR estimation because normally intensity and distribution of noise is unknown. So simplifying assumptions must be made to derive SNR values from noisy image signals.

A posteriori SNR estimation can be done using the values of maximum correlation or grey level differences (FÖRSTNER, 1982; TRINDER, 1982). But doing so, we cannot avoid incorrect correlation. Therefore we need an a priori noise estimation.

We assume that all superposed disturbance effects can be regarded as white noise n , i.e. having a constant power spectrum

$$P_n(f) = N_0^2 \quad (8)$$

P_n is the noise power spectrum, N_0^2 the constant intensity. A typical power spectrum P_g of image and noise is shown in fig.10.

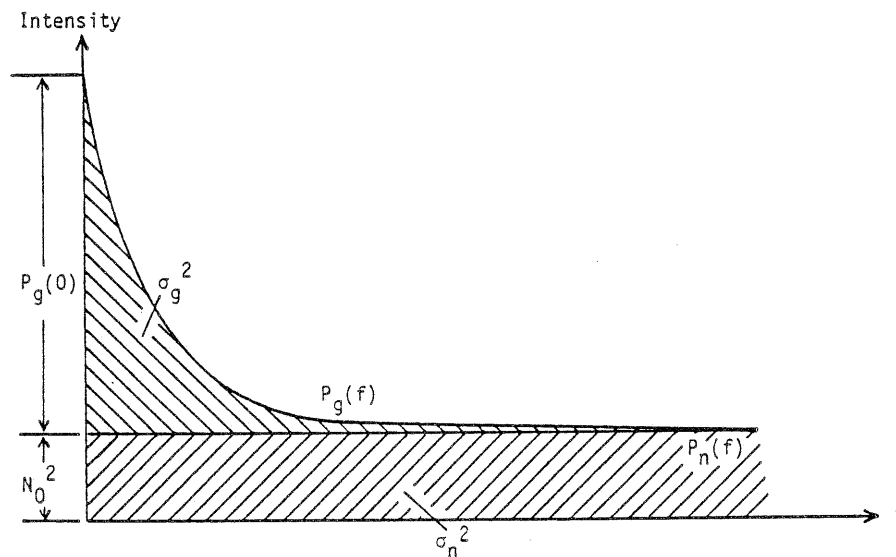


Fig.10: Power spectrum of image and noise

The variances σ_n^2 for noise can be estimated by

$$\sigma_n^2 = N_0^2$$

So σ_n^2 can be estimated in a representative image part according to (8). This σ_n^2 is considered to be valid for all correlation windows. Image and noise can be regarded as independent stochastic variables. Hence the variance σ_g^2 of the undisturbed signal g can be calculated as difference of $\sigma_{g'}^2$, the variance of the disturbed signal g' , and σ_n^2 .

$$\sigma_g^2 = \sigma_{g'}^2 - \sigma_n^2 = \sigma_{g'}^2 - N_0^2$$

So simple variance computation in a correlation window yields the corresponding SNR:

$$\text{SNR} = \sqrt{\frac{\sigma_{g'}^2 - N_0^2}{N_0^2}} \quad (9)$$

Equation (9) is used to estimate the a priori probability P to avoid wrong correlation.

Small scale distortion effects

Another part of the statistical test was to find the effects of small scale image distortions on the correlation probability. Here pixel displacement of fractional pixel size are considered. Pixel distortions are simulated by anisotropic (translation) and isotropic (rotation) spatial filtering. The translation filter matrices can be written as

$$\begin{pmatrix} (1 - dx)dy & dx dy \\ (1 - dx)(1 - dy) & dx(1 - dy) \end{pmatrix}$$

with (dx, dy) the displacement vector in x- and y-direction $(-0.5 \leq dx, dy \leq +0.5)$. The filter matrices associated with pixel rotation α can be denoted as $(-\pi/4 \leq \alpha \leq +\pi/4)$:

$$\begin{pmatrix} 0 & a & 0 \\ a & b & a \\ 0 & a & 0 \end{pmatrix}$$

with $a = (\cos\alpha + \sin\alpha - 1)^2/4 \cdot \sin^2\alpha$
und $b = 1 - 4a$.

The test results solely effect the geometric precision but not the probability of the correlation functions. Without superimposed noise only 2 test results ($\sim 0.02\%$) show deviations more than 1.0 pixel. Only the geometric precision is influenced by pixel distortions. With additional noise the correlation probability does not differ significantly from the results obtained without translation and rotation. So equation (7) and table 3 can be applied as well.

Conclusions

With the presented formulae for correlation probability and image SNR an a priori estimation of the expected correlation accuracy can be given. According to the image quality in a correlation window it is possible to decide which objective function should be used and to calculate the probability of correct (or wrong) correlation.

If a correlation point shows too low SNR, it can be neglected or the SNR (and the correlation probability) can be increased by low pass filtering or by extending the correlation window (EHLERS, 1983). According to (7) correlation probability is referred to only one reason: the SNR. All known methods to raise correlation probability, e.g. filtering or enlargement of the correlation window are doing nothing else but increasing the local SNR at the correlation point. The values of the correlation maxima have no influence on the correlation probability. This corresponds with previous results (EHLERS, 1982a).

Naturally this study tries to answer only one question about correlation quality. Simplifying assumptions for noise and signal have to be made to derive an analytical expression for probability and SNR. Only small geometrical differences have been considered and different quantization errors have not been investigated. Finally the definition of SNR includes only the image variances neglecting such important features as texture parameter, edge direction, significant pattern etc. Therefore SNR-definition should be generalized in this sense.

One main result of this paper is that we must consider objective functions other than solely the normal correlation coefficient. The phase correlation method shows less susceptibility against low SNR and should therefore be applied in noisy images. So future correlation systems should be open to include these and prospective results. They should

contain the opportunity to generalize the objective function, i.e. the metrics and the transformation operator. Also picture preprocessing and variable choice of window size should be feasible. This is only possible on a software solution conveniently embedded into a digital image processing system.

References

- BAILEY, H., E.BLACKWELL, C.LOWERY and J.RATKOVIC (1976): Image Correlation, Part I, Rand Corporation, R-2057/1 - PR, 53 p.
- CASTLEMAN, K. (1979): Digital Image Processing, Prentice Hall, 429 p.
- DENNERT-MÖLLER, E., M.EHLERS, D.KOLOUCH, P.LOHMANN (1982): Das digitale Bildverarbeitungssystem MOBI-DIVAH, Bildmessung und Luftbildwesen 50, pp.201-203
- EHLERS, M. (1982a): Increase in Correlation Accuracy by Digital Filtering, Photogrammetric Engineering and Remote Sensing, Vol.48, pp.415-420
- EHLERS, M. (1982b): Digital Image Processing of Remote Sensing Imagery: A Comparative Study on Different Functions in Correlation Process, Proc.of the Intern.Symp. Comm.VII, ISP, Toulouse, pp.71-77
- EHLERS, M. (1983): Untersuchungen von digitalen Korrelationsverfahren zur Entzerrung von Fernerkundungsaufnahmen, Dissertation, Hannover
- FÖRSTNER, W. (1982): On the Geometric Precision of Digital Correlation, Proc. of Comm.III, ISP, Helsinki, pp.176-189
- GÖPFERT, W. (1980): Image Correlation and Change Detection, Proc.of XIV Congress of ISP, Vol.23/B3, Comm.III, pp.246-255
- KONECNY, G. (1976): Mathematical Models and Procedures for the Geometric Restitution of Remote Sensing Imagery, Working Group Rep.III.1, XIII Congress of ISP, Helsinki
- KUGLIN, C.D. and D.C.HINES (1975): The Phase Correlation Image Alignment Method, Proceedings of the IEEE International Conference on Cybernetics and Society, S.163-165
- PRATT, W.K. (1974): Correlation Techniques of Image Registration, IEEE Transactions on Aerospace and Electronic Systems, Vol.AES-10, pp.353-358
- TRINDER, J.C. (1982): The Effects of Photographic Noise on Pointing Precision, Detection and Recognition, Photogrammetric Engineering and Remote Sensing, Vol.48, pp.1563-1575
- WHISTON, T.G. (1974): Life is Logarithmic, Advances in Cybernetics and Systems, Gordon and Breach